Andean Geology 45 (2): 229-248. May, 2018
doi: 10.5027/andgeoV45n2-3015

Andean Geology
www.andeangeology.cl

Internal framework and geochemistry of the Carboniferous Huaco granite pluton, Sierra de Velasco, NW Argentina

***Fernando G. Sardi [1], Pablo Grosse[2], Mamoru Murata[3], Rafael Pablo Lozano Fernández[4]**

[1] *Instituto Superior de Correlación Geológica (INSUGEO-CONICET), Miguel Lillo 205 (4000), San Miguel de Tucumán, Argentina. fgsardi@csnat.unt.edu.ar*

[2] *Consejo Nacional de Investigaciones Científicas y Técnicas (CONICET) and Fundación Miguel Lillo, Miguel Lillo 251 (4000), San Miguel de Tucumán, Argentina. pablogrosse@yahoo.com*

[3] *Naruto University of Education, Department of Geosciences, 7772-8502, Tokushima, Japan. atarumm@naruto-u.ac.jp*

[4] *Museo Geominero, Instituto Geológico y Minero de España, Ríos Rosas 23, 28003, Madrid, Spain. r.lozano@igme.es*

* *Corresponding author: fgsardi@csnat.unt.edu.ar*

ABSTRACT. The A-type Huaco granite pluton of the Velasco range (Sierras Pampeanas of northwest Argentina) is formed by three coeval granitic facies and contains subordinate coeval-to-late facies, as well as enclaves, dikes and stocks that show different temporal relations, textures and compositions. The dominant facies (Regional Porphyritic Granite; RPG) is a porphyritic two-mica monzo- to syenogranite, with abundant microcline megacrysts up to 12 cm in size. It was emplaced in a dominant extensional setting and has a mainly crustal source but with participation of a mantle-derived component. The RPG transitions towards two coeval and co-genetic granite facies, at its margins (Border Granite; BG) and around Be-pegmatites (Adjacent Porphyritic Granite; APG). These two facies have a finer-grained texture and smaller and less abundant megacrysts. They are also monzo- to syenogranites, but a slight decrease in the biotite/muscovite ratio is observed from the BG to the RPG to the APG. Trace element modeling suggests that the RPG, BG and APG differentiated from the same magma source by fractional crystallization. Temporally older mafic (ME) and felsic (FE) enclaves are common in the pluton. The ME can be considered partially assimilated remnants of a mafic component in the genesis of the RPG, whereas the FE seem to be remnants of premature aplites. Other subordinate rocks intrude the RPG and are, hence, temporally younger: felsic dikes (FD), dioritic dikes (DD) and equiganular granites (EqG) are clearly posterior, whereas coeval-to-late Be-pegmatites (BeP) and orbicular granites (OG) formed during the final stages of crystallization of the pluton. The BeP, OG and FD indicate the presence of abundant water and volatiles. The EqG form small stocks that intrude the RPG and were possibly originated from purely crustal sources. The DD probably correspond to a younger unrelated episode of mafic magmatism.

Keywords: Granitic facies, REE and LIL composition, Fractional crystallization model, Huaco granite, Velasco range, Sierras Pampeanas.

RESUMEN. Estructura interna y geoquímica del plutón granítico carbonífero de Huaco, Sierra de Velasco, NW de Argentina. El Plutón Huaco, ubicado en la sierra de Velasco (en Sierras Pampeanas del noroeste de Argentina), es de afinidad granítica A y está conformado por tres facies graníticas y contiene varias rocas ígneas subordinadas, las que muestran diferentes relaciones temporales, texturas y composiciones. La facies granítica dominante (Granito Porfírico Regional; RPG) es un monzo-sienogranito de dos micas, de textura porfírica con abundantes megacristales de microclino que pueden alcanzar hasta 12 cm de longitud. Ha sido emplazado en un marco tectónico dominantemente extensional y habría tenido una fuente de origen cortical pero también con participación de componentes mantélicos. En los bordes del Plutón Huaco y envolviendo a pegmatitas de berilo contenidas en el mismo (BeP), se reconocen las facies cogenéticas BG y APG respectivamente, las cuales tienen contacto transicional con el RPG. Estas dos facies tienen textura de grano

más fino y megacristales de menor tamaño y menos abundante que la unidad principal RPG. También son de composición monzo-sienogranítica y se observa un decrecimiento de la relación biotita/muscovita en el sentido BG-RPG-APG. Estas tres facies graníticas cogenéticas habrían sido formadas por procesos de cristalización fraccionada a partir de un mismo magma de acuerdo al modelado geoquímico utilizando elementos traza. Además, el plutón contiene enclaves máficos (ME) y félsicos (FE) los cuales se formaron temporalmente con anterioridad a la facies granítica dominante. Los ME pueden ser considerados como remanentes asimilados de un componente máfico durante la génesis del RPG, mientras que los FE podrían corresponder a remanentes de aplitas prematuras. Otras rocas subordinadas intruyen al RPG y por lo tanto son consideradas temporalmente posteriores: diques félsicos (FD), diques dioríticos (DD) y granitos de texturas equigranulares (EqG) son claramente posteriores, mientras que las BeP y un granito orbicular (OG) se formaron durante los estadios finales de cristalización del plutón. Las BeP, OG y FD indican la presencia de abundante agua y volátiles. Los EqG forman pequeños stocks que intruyen al RPG y se habrían formado a partir de una fuente puramente cortical. Los DD probablemente correspondan a un episodio independiente más joven de magmatismo máfico.

Palabras clave: Elementos trazas, Modelo de cristalización fraccionada, Facies granítica, Granito Huaco, Sierra de Velasco, Sierras Pampeanas.

1. Introduction

Granitic plutons usually display compositional and/or textural heterogeneities at different scales and magnitudes, which are commonly referred to as internal "facies". Besides, temporally previous/early and/or posterior/later magmatic rocks are commonly included within the main or dominant granitic facies. In the field, these subordinate rocks are found as dikes, enclaves, small stocks, pegmatites, lenses or pods, or irregular bodies of varying dimensions, with either sharp or diffuse contacts with the main granitic facies. The study of these subordinate rocks and their relationships with the main granitic facies can give insights into the processes that formed the pluton and its magmatic evolution (*e.g.,* Smith *et al*., 1999; Breiter *et al*., 2005; Černý *et al*., 2005).

An example of such plutons with a varied internal framework is the Lower Carboniferous Huaco Pluton, part of the Velasco Range in the Sierras Pampeanas of NW Argentina. It is formed predominantly of porphyritic syeno- to monzogranites and contains several distinct subordinate facies and associated magmatic rocks with variable morphologies, compositions, textures and temporal relations. Several previous studies have described the main features of this pluton and some of its minor facies (Grosse and Sardi, 2005; Grosse *et al*., 2009; Sardi *et al*., 2010, 2011; Dahlquist *et al*., 2010, 2013) as well as some of the associated rocks, for example, Be-pegmatites (Cravero, 2005; Sardi *et al*., 2015), an orbicular granite (Quartino and Villar Fabre, 1962; Grosse *et al*., 2010) and the La Chinchilla stock (Grosse *et al*., 2005, 2009; Macchioli Grande *et al*., 2015). However, none of these previous studies have considered all of the facies and associated magmatic rocks and their temporal and genetic links. In this paper, we revise and present new field, petrographic and geochemical data for each of the facies and related magmatic rocks of the Huaco pluton, in order to determine their distinctive features and deduce the genetic links among them.

2. Geology of the Velasco Range

The Velasco range, located in La Rioja province of NW Argentina (Fig. 1a), is one of the largest ranges of the Sierras Pampeanas geologic province, which is characterized by extensive outcrops of crystalline basement composed of Upper Precambrian to Ordovician metamorphic rocks (*e.g.,* Rossi *et al*., 2002; Larrovere *et al*., 2011) and Ordovician to Lower Carboniferous igneous, mainly granitoid, rocks (*e.g.,* Toselli *et al*., 1986, 2002; Rapela *et al*., 2001; Dahlquist *et al*., 2010, 2013; Alasino *et al*., 2012).

The Velasco range is formed essentially by granitoids (Grosse *et al*., 2003, 2011; Báez *et al*., 2005; Toselli *et al*., 2005, 2006). Only a small portion of the range is occupied by outcrops of low to high grade metamorphic rocks, which are recognized as the La Cébila Formation (González Bonorino, 1951) and more recently as the La Cébila Metamorphic Complex (LCMC; Verdecchia, 2009), of Early (-Middle) Ordovician age (Verdecchia *et al*., 2007, 2011) (Fig. 1b). The metamorphic rocks consist of a sequence of phyllites, meta-quartzites, and minor micaceous and quartz-micaceous schists, gneiss and migmatites (Verdecchia and Baldo, 2010; De Los Hoyos *et al*., 2011; Larrovere *et al*., 2012).

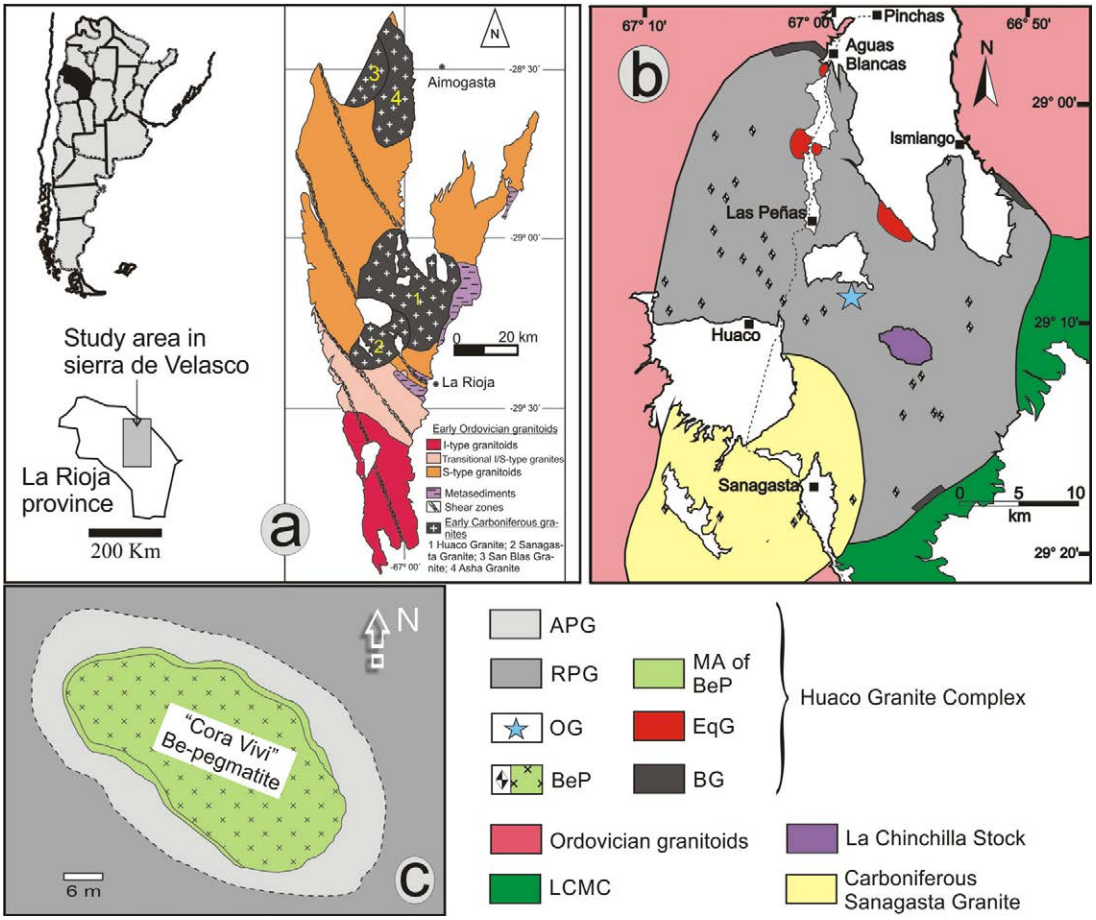

FIG. 1. **a**. Simplified geologic map of the sierra de Velasco (taken to Grosse *et al*., 2011); **b.** Geological map of the study area, NW Argentina, modified from Sardi *et al*. (2010); **c.** Cora Vivi Be-Pegmatite as example to show specifically the APG and MA facies. **RPG:** Regional Porphyritic Granite; **BG:** Border Granite; **APG:** Adjacent Porphyritic Granite; **BeP:** Be-pegmatite; **MA:** Marginal Aplite of the Be-Pegmatite; **EqG:** Equigranular Granites; **OG:** Orbicular granite; **LCMC:** La Cébila Metamorphic Complex.

Two pulses of magmatism are found in the Velasco range, Ordovician and Lower Carboniferous (Pankhurst *et al*., 2000; Toselli *et al*., 2007; Dahlquist *et al*., 2013). The Ordovician magmatic episode, linked to the Famatinian magmatic arc (*e.g.,* Pankhurst *et al*., 1998), originated peraluminous S-type porphyritic granitoids on the northwestern and western flanks of the Velasco range, and metaluminous to weakly peraluminous I-type granodiorites and tonalites on the southern portion of the range (Bellos, 2005; Rossi *et al*., 2005a; Grosse *et al*., 2011; Bellos *et al*., 2015). The Ordovician granitoids were affected by dynamic metamorphism that generated NNW-SSE-trending ductile shear zones of regional extension. Shear zones dated at neighboring ranges constrain the timing of deformation to the Silurian-Early Devonian (*e.g.,* Höckenreiner *et al*., 2003) (Fig. 1a).

The Lower Carboniferous magmatic episode produced post-tectonic granites that intrude the deformed Ordovician granitoids and metamorphic rocks of the LCMC. In the northern part of the range, the Asha and Santa Cruz granites have yielded ages of 361±4 and 354±4 Ma (U-Pb on monazite, Toselli *et al*., 2011), whereas the San Blas pluton has yielded an age of 340±3 Ma (U-Pb on zircon, SHRIMP, Dahlquist *et al*., 2006). In the central part of the range (Fig. 1b), the Huaco and Sanagasta granites have yielded ages of 350 to 358 Ma and 353±1 Ma, respectively (U-Pb on monazite; Grosse *et al*., 2009).

3. Huaco Granite Pluton

The sub-ellipsoidal (~40x30 km) Huaco granite pluton occupies an area of around 620 km^2 in the central-eastern part of the Velasco range (Fig. 1a, b). It is formed predominantly by two-mica porphyritic syeno- to monzogranites (Huaco granite *s.l.*; Grosse and Sardi, 2005; Grosse *et al*., 2009). It is in contact to the SW with another Lower Carboniferous pluton, the Sanagasta granite pluton (Grosse *et al*., 2009) (Fig. 1b).

Grosse *et al*. (2009) determined that the main facies of the Huaco granite is silica- and potassium-rich, ferroan, alkali-calcic to slightly calc-alkalic, and moderately to weakly peraluminous (ASI: 1.06-1.18). Furthermore, Grosse *et al*. (2009) concluded, based on isotopic data, that the Huaco granite has a mainly crustal source, but with some participation of a more primitive, possibly mantle-derived, component. The Huaco granite pluton has several characteristics indicating it is an A-type granite (*e.g.,* Collins *et al*., 1982; Whalen *et al*., 1987; Eby, 1990, 1992): ferrous affinity (high Fe/Mg ratios), low CaO, Sr and Ba contents, high contents in trace elements such as Ga, Nb, Ta, Y and HREE, and high FeO/MgO ratios (Abdel Rahman, 1994) and F and Cl contents (Muñoz, 1984) in biotites (Grosse, 2007; Grosse *et al*., 2009; Dahlquist *et al*., 2010). However, the geochemical composition of the pluton is more compatible with a post-orogenic environment than with an anorogenic environment (Grosse, 2007; Grosse *et al*., 2009).

Both the Huaco and Sanagasta granites are host to the Be-pegmatites of the Velasco Pegmatitic District (Sardi *et al*., 2002, 2015). The geochemical evolutionary trend from the main facies of the Huaco granite towards the Be-pegmatites has been studied by Sardi *et al*. (2010, 2011). The Huaco granite consists of several facies and associated rocks which are described in the next section.

4. Internal Lithological Framework of the Huaco Granite Pluton

4.1. Occurrence and petrography

The Huaco granite pluton is composed of a main and dominant porphyritic facies, previously studied by several authors (see above). Following Sardi *et al*. (2010), we name the main facies Regional Porphyritic Granite (RPG). This main facies transitions towards two coeval facies, at the margins of the pluton (Border Granite; BG) and around Be-pegmatites (Adjacent porphyritic granite; APG) (Figs. 1c and 2a). Two more facies found within the main RPG can be considered as coeval-to-late facies (Fig. 1b, c and a): Be-pegmatites (BeP) and an orbicular granite pod (OG).

In addition, other magmatic rocks are included in the Huaco granite pluton and can be temporally identified as early or posterior units spatially related to the main facies (RPG). The former are enclaves of either mafic (Mafic Enclaves; ME) or felsic compositions (Felsic Enclaves; FE), whereas the posterior rocks are mafic dikes (Dioritic Dikes; DD), felsic dikes (Felsic Dikes; FD) and equigranular leucogranite intrusive stocks (Equigranular Granites; EqG), including the La Chinchilla stock (Figs. 1b and 2b).

4.1.1. The main facies (RPG)

Regional Porphyritic Granite (RPG): it consists of syeno- to monzogranites with a porphyritic texture resulting from abundant idiomorphic microcline megacrysts immersed in a medium to coarse grained equigranular groundmass (Fig. 3a). The megacrysts reach sizes of up to 12 cm and their abundance varies between 24 and 39%. The mineralogy is quartz (25-39%), usually twinned plagioclase (18-31%), twinned and often perthitic interstitial microcline (2-14%), biotite (4-10%) with inclusions of zircon and apatite, muscovite (2-6%), idiomorphic apatite (up to 0.5%) and zircon, monazite, opaque minerals, and occasionally fluorite (<1%) (Grosse *et al*., 2009).

4.1.2. The coeval facies (BG and APG)

These facies have been studied previously by Sardi *et al*. (2010 and 2011). They include:

Border Granite (BG): this is the marginal facies of the RPG and occurs in the northern and eastern margins of the Huaco granite pluton (Fig. 1b). It is approximately 100 m wide and grades transitionally towards the RPG (Fig. 2a). The BG is characterized by a finer-grained groundmass and smaller and less abundant megacrysts compared to the RPG (Fig. 3b). Its mineralogy is quartz (34-40%), twinned and zoned plagioclase (23-34%), twinned and perthitic microcline (19-33%), biotite (5-7%) and muscovite (2-4%). Apatite, zircon and opaque minerals are usually included in biotite (Sardi *et al*., 2011).

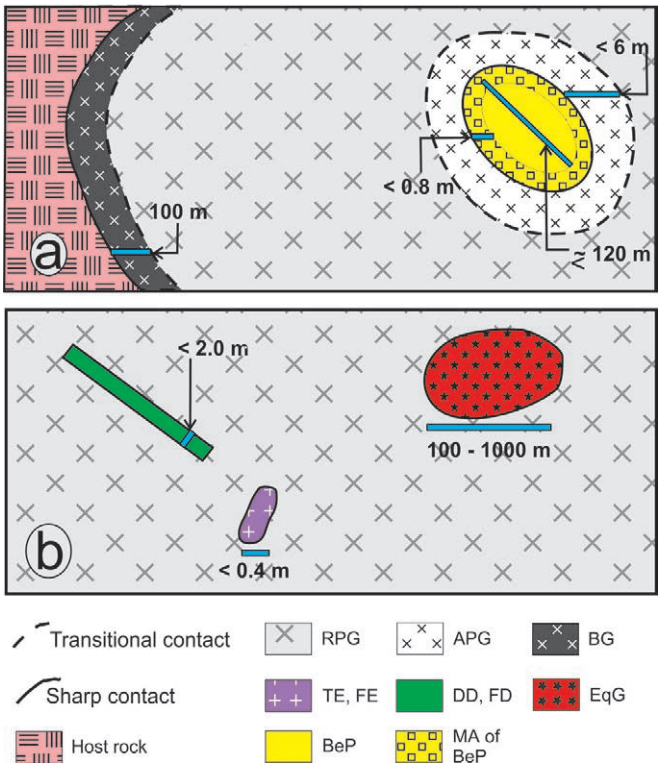

FIG. 2. Schematic graphical representation of the different facies and associated rocks found in the Huaco granite pluton, Velasco range, NW Argentina. **a.** RPG, BG, APG, BeP and MA; **b.** RPG, ME-FE, DD-FD and EqG. **RPG:** Regional Porphyritic Granite; **BG:** Border Granite; **APG:** Adjacent Porphyritic Granite; **ME:** Mafic Enclave; **FE:** Felsic Enclave; **BeP:** Be-pegmatite; **MA:** Marginal Aplite of the Be-Pegmatite; **DD:** Dioritic Dike; **FD:** Felsic Dike; **EqG:** Equigranular Granites.

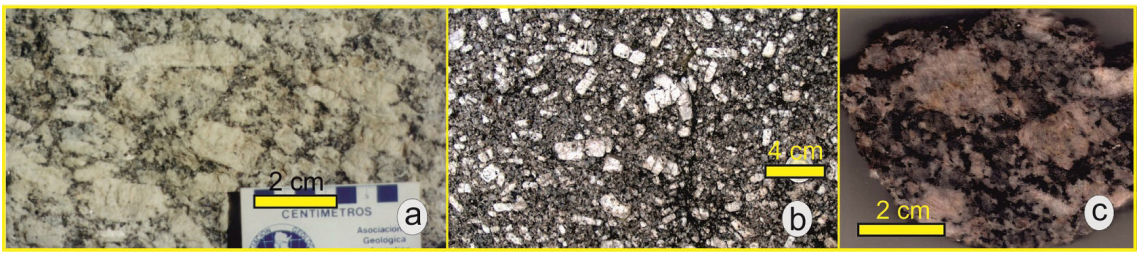

FIG. 3. Macroscopic texture of the main and coeval facies. **a.** RPG (taken from Sardi *et al*., 2015); **b.** BG; **c.** APG.

Adjacent Porphyritic Granite (APG): this facies surrounds the Be-pegmatites for distances not greater than 6 m from the pegmatite margins (Fig. 2a). Similar to the BG, the APG also has a finer-grained groundmass and less abundant (average value ~29%) and smaller (<4 cm) microcline megacrysts compared to the RPG (Fig. 3c). Also, it has higher quartz (28-56%) and microcline (26-52%) contents and less plagioclase (10-24%). A slight increase of muscovite and a decrease of biotite are also observed. Minor phases are apatite, zircon, monazite, and occasionally fluorite.

4.1.3. The coeval-to-late facies (BeP and OG)

Be-pegmatites (BeP): they are lens-shaped with the main axis length up to 140 m (Sardi *et al*., 2015).

They are commonly zoned, showing an aplitic or leucogranitic border zone, an intermediate pegmatitic zone composed mainly of K-feldspar and accessory minerals (beryl, apatite, triplite and muscovite), and a quartz core. The outer thin rim of the Be-pegmatites (Marginal Aplite of the Pegmatites, or MA, following Sardi *et al*., 2010) is in sharp contact with the APG and usually grades inward towards the Be-pegmatite zone. It commonly consists of aplites or more rarely of muscovite-rich equigranular leucogranites. The width of the MA is variable, but not greater than 0.8 m. Its mineralogy is quartz (35-44%), perthitic microcline and twinned plagioclase in similar amounts (16-27% and 19-33%, respectively); muscovite (≤10%) is the main accessory mineral, whereas biotite is scarce and sometimes absent; fluorite is recognized occasionally (around 1%). Columbite-tantalite is occasionally found (Sardi *et al*., 2015).

Orbicular Granite (OG): it is a small (65x15 m), irregularly shaped body located in the central part of the Huaco pluton (Fig. 1b). It has been studied by Quartino and Villar Fabre (1962) and Grosse *et al*. (2010). The OG consists of ellipsoid-shaped orbicules of 3 to 15 cm immersed in an aplitic-pegmatitic matrix. The orbicules consist of a core formed by a K-feldspar megacryst, partially to totally replaced by plagioclase, and alternating layers of radial and plumose plagioclase crystals and tangentially oriented biotite rings (Grosse *et al*., 2010). Grosse *et al*. (2010) conclude that the orbicular granitoid formed *in situ* in a pocket of evolved and volatile-rich melt segregated from the surrounding partially crystallized Huaco granite, possibly via a filter pressing mechanism.

4.1.4. Enclaves (ME and FE)

Mafic Enclaves (ME): they are dark and small, with sizes mostly under 20 cm (Fig. 4a), and rarely up to 50 cm. They usually have rounded and oval shapes, occasionally being very stretched-out parallel

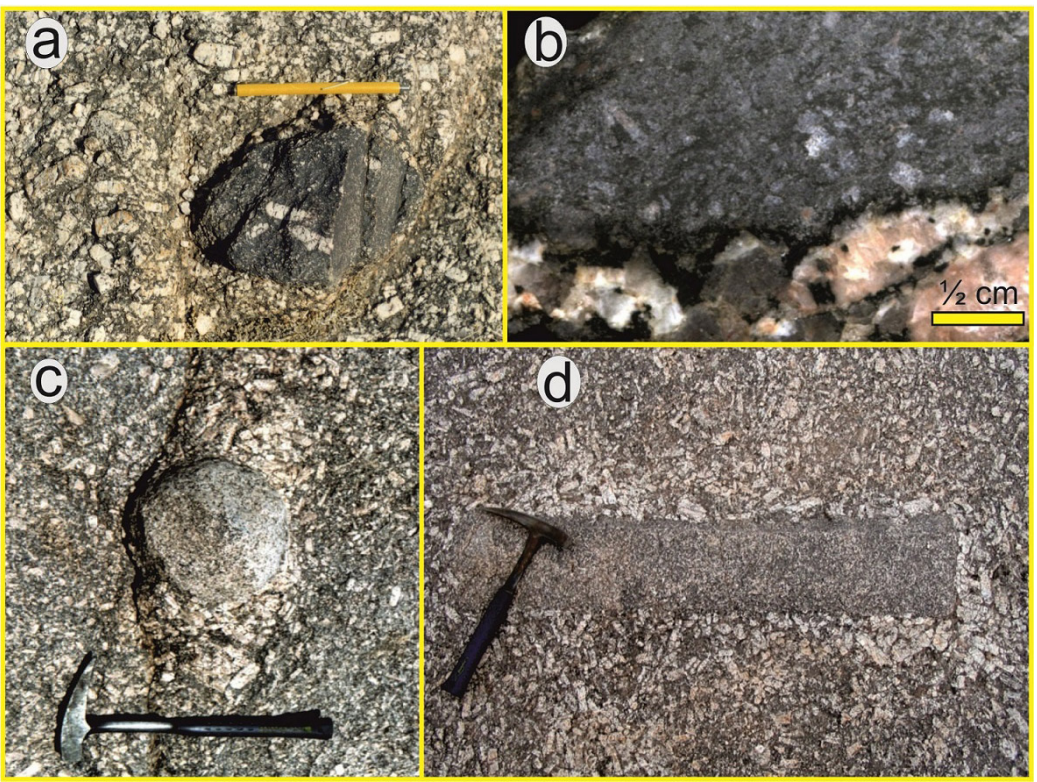

FIG. 4. Mafic and felsic enclaves within the Huaco granite pluton (RPG facies). **a-b.** ME, showing assimilation of megacrystals of microcline from host-rock; **c-d.** FE with rounded and rectangular shape, respectively; in both examples the RPG megacrsyts accumulate around the enclaves.

to the magmatic flow. The contact with the host RPG is sharp. They commonly contain xenocrysts and xeno-megacrysts probably incorporated from the host granite magma (Fig. 4a and b).

The ME have predominantly tonalite compositions and fine-grained equigranular textures (0.1 to 0.5 mm). They are very rich in biotite, varying in abundance from 10% to 50%. Apatite is relatively abundant and is found as elongated prisms and needles included mostly in quartz and plagioclase. The content of opaque minerals is roughly proportional to the abundance of biotite and ranges from ~1% to 10%; pyrite, ilmenite and magnetite have been identified.

Felsic Enclaves (FE): these enclaves can reach 2 m in size. They have irregular or oval shapes and rounded borders (Fig. 4c), or more rarely straight sides (Fig. 4d). They are gray to light pink with equigranular textures, either fine-grained (0.3-1.5 mm) or fine-to-medium-grained (0.7-5.0 mm). Commonly, the microcline megacrystals of the RPG accumulate around the FE (Fig. 4 c, d), suggesting an early formation for the enclaves.

Felsic enclaves are syenogranites with quartz (33-34%) and perthitic microcline (41-45%). Both minerals are xenomorphic. Plagioclase (15-19%) is found as small subidiomorphic twinned crystals. Muscovite is the main accessory mineral (5-7%) while biotite is scarce (<2%). Apatite and zircon are very scarce and are included in biotite.

4.1.5. Dikes (DD and FD)

Dioritic Dikes (DD): according to field observations of Grosse (2007) and Dahlquist *et al*. (2010), the Huaco granitic pluton is cut by scarce dioritic dikes. They are black, fine grained (0.1-0.3 mm), up to 3 m wide and are in sharp contact with the RPG. Twinned sub-idiomorphic plagioclase is the most abundant mineral, commonly altered to sericite. Mafic minerals are found in an abundance of 20 to 30%. Biotite is the most abundant of them and it is found as subhedral sheets with typical pleocroism, generally altered to chlorite. Other mafic minerals present are hornblende, titanite and opaque minerals. Apatite forms small elongated prisms and needles, although in smaller abundances than in mafic enclaves. Secondary calcite is also observed.

Felsic Dikes (FD): they are usually straight and are in sharp contact with the RPG (Fig. 5a and b). They are aplitic (20-30 cm in width), (Fig. 5a) with a fine-grained equigranular texture (0.1 to 1.5 mm), although one slightly porphyritic leucogranitic dike was found (<2 m in width) (Fig. 5b). They are monzogranitic, with quartz (31%), microcline (28-32%) and plagioclase (27-35%) as essential minerals, and muscovite (6-10 %) as the main accessory mineral; biotite is very scarce (<1%).

The leucogranitic dike contains small microcline megacrysts (size ~1.3 cm; proportion ~10%) immersed in a medium to fine-grained equigranular matrix. The modal composition is quartz (46%), microcline (29%), plagioclase (19%), biotite and muscovite (<2%). Garnet (~4%) has been identified in this dike; it is idiomorphic, with variable sizes from small crystals to 2.5 mm.

4.1.6. Equigranular granites (EqG)

Equigranular Granites (EqG): the EqG (Fig. 5c) are small bodies or stocks that intrude the RPG (Fig. 5d). Their sizes vary from very small (<100 m diameter) to larger stocks of more than 1 km^2. They have irregular shapes and usually sharp contacts (Fig. 5e).

The EqG are felsic two-mica monzogranites (muscovite>biotite). The quartz and microcline crystals have similar sizes, between 1-3 mm. Quartz (26-43%) form xenomorphic crystals. Plagioclase (25-35%) has sub-idiomorphic habit and polysynthetic twinning. Microcline (23-29%) is xenomorphic and twinned after pericline-albite law. Muscovite (2-9%) is generally more abundant than biotite (1-5%). Tourmaline is found in abundances of up to 1% in some EqG bodies. Apatite, zircon and monazite are very scarce.

The La Chinchilla stock (Fig. 1b) is a particular EqG that has received special attention because of its high U content (Grosse *et al*., 2005, 2009; Salvatore *et al*., 2011, 2013; Parra *et al*., 2011; Morello and Aparicio González, 2013). It is a medium-grained equigranular to slightly porphyritic leucogranite (Grosse *et al*., 2005, 2006 and 2009) that clearly intrudes the RPG. Its mineralogy consists of quartz, plagioclase, K-feldspar, biotite, fluorite, zircon, monazite, occasional beryl and very scarce apatite.

4.2. Geochemistry

Geochemical analysis is based on 35 representative samples of the different facies of the Huaco granite pluton and associated magmatic rocks: 8 of the

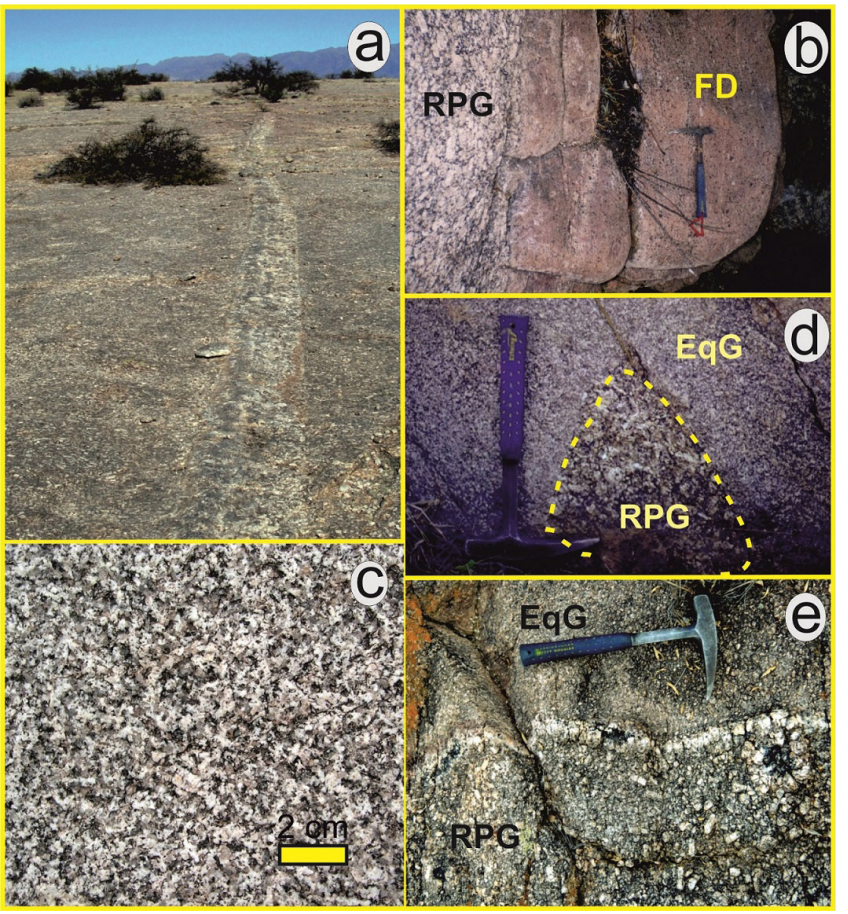

FIG. 5. Posterior facies. **a.** FD, straight aplite dike; **b.** FD, garnet-bearing slightly porphyritic granitic dike; **c.** Equigranular granite EqG; **d.** Enclave of RPG in an EqG; **e.** Sharp contact between RPG and an EqG.

RPG; 2 of the BG; 7 of the APG; 4 of the MA; 6 of the ME; 3 of the FE; 1 of the DD; 2 of the FD and 2 of the EqG. The analyses were performed at the laboratories of IGME (Instituto Geominero de España), Naruto University of Education (Japan), Huelva University (Spain) and ACTLAB (Canada). Major elements were determined by XRF, and trace elements by ICP-MS/AES. The analyses are shown in table 1, and include our new data (n=8) together with previously unpublished analyses of Grosse (2007; n=7) and published data of both Grosse *et al*. (2009; n=5) and Sardi *et al*. (2010; n=15).

4.2.1. Major elements and Rb, Sr, Ba and Cs compositions

Granitoids: the facies and associated rocks of granitic composition are silica-rich, with SiO_2 mostly between 68 and 75%; two samples with higher contents of 78 and 81% belong to FD and MA, respectively. All rocks are peraluminous (ASI >1, average 1.16). The FeO_t and TiO_2 contents are higher in the main and coeval facies (RPG, BG and APG) (FeO_t>1.7%; TiO_2 ≥0.20%) than in the other rocks (FeO_t <1.7% and TiO_2 ≤0.20%). This distinction is not so evident for MgO, as the 2 EqG and the 2 FE samples are within the range of the main and coeval facies. K_2O >Na_2O for all cases except for two MA samples. K_2O+Na_2O is between 7.4 and 9.4% for the RPG, APG and BG facies, between 5.6 and 8.4% for the MA, and between 8.4 and 9% for the other rocks.

All samples are rich in FeO_t in relation to MgO, with FeO_t/FeO_t+MgO ratios >0.79 (wt%) (Fig. 6a). Most samples plot in the ferroan field of "A-type granites" in the diagram of Frost *et al*. (2001) (Fig. 6a)

TABLE 1. REPRESENTATIVE CHEMICAL COMPOSITION OF THE HUACO GRANITE PLUTON.

Sample		SiO_2	TiO_2	Al_2O_3	FeO_t	MnO	MgO	CaO	Na_2O	K_2O	P_2O_5	LOI	Total	ACNK	Cs	Ba	Rb	Sr	Rb/Sr	Ba/Rb
RPG	**6587**	73.94	0.23	13.22	2.31	0.07	0.24	0.88	2.88	5.32	0.15	0.98	100.2	1.09	36.6	185	457	46.0	9.93	0.40
	6590	73.99	0.22	12.81	2.05	0.04	0.30	0.91	2.79	4.91	0.22	0.96	99.20	1.11	21.1	181	343	48.0	7.15	0.53
	6619	69.80	0.40	14.38	3.02	0.06	0.41	1.51	3.12	5.46	0.40	1.16	99.72	1.04	19.8	301	369	73.0	5.05	0.82
	6650*	72.48	0.43	13.48	3.02	0.06	0.49	1.10	3.01	4.69	0.34	nd	99.10	1.12	39.6	203	390	60.0	6.50	0.52
	6746*	68.06	0.53	14.31	3.88	0.09	0.60	1.22	3.14	4.92	0.40	nd	97.15	1.13	nd	187	480	54.4	8.82	0.39
	6748*	70.94	0.28	14.85	2.29	0.06	0.28	0.86	3.43	5.32	0.26	nd	98.57	1.15	51.8	204	412	52.4	7.86	0.50
	6846*	70.92	0.29	14.26	2.29	0.07	0.26	1.12	3.35	5.65	0.27	nd	98.48	1.04	nd	256	361	66.2	5.45	0.71
	6847*	70.86	0.31	14.27	2.40	0.06	0.39	0.75	2.95	5.63	0.31	nd	97.93	1.16	54.2	208	429	50.5	8.50	0.48
BG	**6931[a]**	71.99	0.29	14.15	1.73	0.04	0.44	0.88	3.05	5.51	0.25	0.75	99.08	1.12	25.6	368	290	81.3	3.57	1.27
	7697[a]	71.64	0.35	14.19	2.28	0.06	0.38	0.86	3.04	5.59	0.30	0.65	99.35	1.13	31.2	268	282	73.6	3.83	0.95
APG	**6657***	73.23	0.19	13.94	1.68	0.05	0.24	0.62	3.11	5.32	0.22	nd	98.60	1.16	31.5	169	420	43.2	9.72	0.40
	6738*	70.06	0.35	14.63	2.93	0.09	0.41	0.97	3.45	5.25	0.37	nd	98.51	1.11	76.1	213	487	56.0	8.70	0.44
	6744*	73.12	0.30	13.86	2.31	0.06	0.32	0.85	3.34	4.60	0.21	nd	98.97	1.15	nd	181	393	48.5	8.10	0.46
	6842*	72.44	0.24	14.30	1.66	0.06	0.16	0.27	2.20	7.07	0.20	nd	98.60	1.22	113	254	658	43.0	15.3	0.39
	6924*	74.34	0.21	13.20	1.84	0.09	0.20	0.74	2.94	4.50	0.12	nd	98.18	1.19	nd	166	447	37.1	12.1	0.37
	7122*	70.60	0.25	14.18	2.14	0.06	0.32	0.80	3.28	5.94	0.30	nd	97.87	1.07	48.1	223	485	94.8	5.12	0.46
	7129*	70.99	0.22	14.39	1.94	0.05	0.28	0.89	3.52	5.86	0.23	nd	98.37	1.05	21.3	200	403	55.6	7.25	0.50
MA	**6615**	81.16	0.04	10.34	0.50	0.03	0.04	0.17	2.63	2.99	0.14	0.97	99.00	1.31	32.6	28	329	7.00	47.0	0.09
	7121A*	75.01	0.07	14.07	0.65	0.05	0.09	0.60	5.35	3.02	0.26	nd	99.17	1.07	24.0	55	327	16.6	19.7	0.17
	7121B*	73.99	0.06	14.83	0.73	0.04	0.09	0.56	5.22	2.76	0.26	nd	98.54	1.18	32.3	66	376	13.9	27.1	0.18
	7121C*	72.93	0.09	15.01	0.78	0.04	0.10	0.49	4.39	4.39	0.26	nd	98.48	1.17	31.3	83	434	25.0	17.4	0.19
ME	**6649**	51.86	1.50	15.43	8.68	0.13	5.82	5.73	0.83	4.19	0.64	nd	94.81	0.95	nd	1,019	519	768	0.68	1.96
	6745	56.59	0.95	18.09	7.55	0.16	3.04	0.36	0.61	7.09	0.1	nd	94.54	1.94	nd	390	360	26.7	13.5	1.08
	6747	63.62	0.93	15.02	5.71	0.09	2.47	3.28	3.12	2.54	0.16	nd	96.94	1.08	nd	189	220	121	1.82	0.86
	6877[a]	70.49	0.54	14.29	3.72	0.10	0.61	1.17	3.33	4.87	0.42	0.51	100.0	1.11	36.7	136	1,913	43.6	43.9	0.07
	7728[a]	54.94	2.51	14.52	12.44	0.24	2.37	1.82	2.50	4.50	0.85	1.03	97.71	1.18	175	118	2,758	26.5	104	0.04
	7734[a]	62.98	1.19	15.65	7.57	0.14	1.22	2.20	4.41	2.83	0.60	0.74	99.53	1.09	46.9	123	356	48.6	7.33	0.34
FE	**6588**	72.96	0.14	13.17	1.67	0.042	0.22	0.63	2.84	6.06	0.12	0.86	98.71	1.06	11.8	171	376	47.0	8.00	0.45
	6914	74.44	0.12	13.68	1.03	0.03	0.17	0.36	2.55	6.14	0.23	0.60	99.34	1.19	26.9	107	327	26.0	12.6	0.33
	6972	75.20	0.07	13.16	0.67	0.02	0.13	0.35	2.72	6.26	0.21	0.46	99.25	1.11	33.1	100	347	42.3	8.20	0.29
DD	**7742**	56.59	1.73	15.77	8.23	0.15	3.81	4.68	4.15	3.07	0.67	1.63	100.5	0.84	27.8	222	131	477	0.28	1.69
FD	**6589**	78.13	0.02	11.58	0.92	0.11	0.04	0.34	2.75	5.44	0.09	0.43	99.85	1.05	3.90	119	263	37.0	7.11	0.45
	7733	74.37	0.08	13.92	1.03	0.05	0.08	0.33	3.54	4.89	0.13	0.70	99.11	1.19	39.31	78	343	19.8	17.3	0.23
EqG	**7233**	72.39	0.14	14.56	1.20	0.05	0.26	0.54	3.38	5.39	0.32	0.78	99.01	1.18	115	148	382	37.2	10.3	0.39
	7400	72.76	0.20	14.17	1.49	0.04	0.34	0.68	3.29	4.95	0.31	0.74	98.97	1.18	60.0	177	330	48.7	6.77	0.54

table 1 continued.

	Sample	Y	La	Ce	Pr	Nd	Sm	Eu	Gd	Tb	Dy	Ho	Er	Tm	Yb	Lu	LREE	HREE	Eu/Eu*	La_n/Yb_n
RPG	**6587**	65.0	47.4	107	12.8	45.8	10.9	0.82	9.54	1.95	12.0	2.25	5.99	0.97	5.58	0.74	225	39.0	0.25	5.68
	6590	38.0	30.0	86.0	8.27	29.6	6.98	0.73	6.23	1.28	7.36	1.23	2.96	0.44	2.57	0.33	162	22.4	0.34	7.81
	6619	44.4	63.6	139	16.7	62.5	13.4	1.46	10.9	1.83	9.74	1.64	4.11	0.57	3.38	0.44	297	32.6	0.37	12.6
	6650**	38.6	49.4	112	13.6	51.5	11.2	0.94	10.1	1.45	7.48	1.24	3.22	0.40	2.40	0.34	239	26.6	0.27	13.8
	6746**	44.2	nd	nd	nd	nd	nd	nd	nd	nd	nd	nd	nd	nd	nd	nd	-	-	-	-
	6748**	36.2	32.0	73.2	8.72	33.3	7.5	0.87	7.08	1.12	6.25	1.11	3.11	0.43	2.73	0.4	156	22.2	0.37	7.84
	6846**	34.6	nd	nd	nd	nd	nd	nd	nd	nd	nd	nd	nd	nd	nd	nd	-	-	-	-
	6847**	37.7	36.2	82.7	10.0	38.1	8.50	0.85	7.71	1.21	6.47	1.11	2.99	0.40	2.41	0.34	176	22.6	0.32	10.0
BG	**6931**[a]	17.8	42.9	88.7	11.6	52.3	10.5	0.75	7.68	0.85	4.54	0.63	1.71	0.11	1.31	0.08	207	16.9	0.26	21.9
	7691[a]	29.6	34.4	73.0	9.75	38.5	7.66	1.12	6.98	1.17	6.49	1.19	3.26	0.48	2.94	0.45	164	23.0	0.47	7.82
APG	**6657****	35.7	24.3	54.9	6.58	24.2	5.60	0.60	5.27	0.86	4.92	0.85	2.22	0.30	1.85	0.26	116	16.5	0.34	8.78
	6738**	43.3	39.3	87.9	10.8	40.6	8.77	0.97	8.11	1.28	7.02	1.27	3.61	0.49	3.11	0.44	188	25.3	0.35	8.45
	6744**	35.8	nd	nd	nd	nd	nd	nd	nd	nd	nd	nd	nd	nd	nd	nd	-	-	-	-
	6842**	43.8	38.1	85.5	10.3	38.7	8.38	1.03	7.24	1.07	5.1	0.78	1.89	0.24	1.42	0.2	182	17.9	0.41	17.9
	6924**	38.7	nd	nd	nd	nd	nd	nd	nd	nd	nd	nd	nd	nd	nd	nd	-	-	-	-
	7122**	40.1	31.8	71.3	8.77	33.2	7.41	0.79	6.88	1.08	5.99	1.02	2.73	0.36	2.32	0.32	153	20.7	0.34	9.17
	7129**	36.3	28.0	63.5	7.62	28.4	6.66	0.78	6.58	1.14	6.81	1.19	3.17	0.42	2.6	0.36	135	22.3	0.36	7.20
MA	**6615**	4.0	1.58	3.09	0.36	1.13	0.37	0.03	0.31	0.08	0.52	0.09	0.21	0.04	0.3	0.04	6.56	1.59	0.30	3.52
	7121A**	25.2	2.78	5.88	0.68	2.44	0.70	0.13	0.81	0.19	1.39	0.28	0.87	0.14	1.00	0.14	12.6	4.82	0.53	1.86
	7121B**	26.1	1.08	2.33	0.28	1.00	0.34	0.06	0.39	0.10	0.68	0.13	0.41	0.07	0.56	0.08	5.09	2.42	0.51	1.29
	7121C**	29.5	3.42	7.20	0.86	3.04	0.84	0.20	0.93	0.20	1.33	0.26	0.79	0.12	0.92	0.12	15.6	4.67	0.70	2.49
TE	**6649**	41.1	nd	nd	nd	nd	nd	nd	nd	nd	nd	nd	nd	nd	nd	nd	-	-	-	-
	6745	34.3	nd	nd	nd	nd	nd	nd	nd	nd	nd	nd	nd	nd	nd	nd	-	-	-	-
	6747	29.0	nd	nd	nd	nd	nd	nd	nd	nd	nd	nd	nd	nd	nd	nd	-	-	-	-
	6877[a]	33.53	39.11	83.9	12.2	45.6	10.2	0.78	9.28	1.55	8.02	1.45	3.47	0.48	2.64	0.38	192	27.3	0.25	9.90
	7728[a]	49.25	48.76	98.0	15.2	65.1	13.6	1.15	13.3	2.12	11.8	2.16	5.36	0.74	4.25	0.62	242	40.4	0.26	7.68
	7734[a]	51.00	62.70	122	18.7	76.9	15.1	1.32	14.0	2.26	12.0	2.20	5.71	0.80	4.87	0.73	297	42.6	0.28	8.61
FE	**6588**	53.10	26.9	60.4	7.15	28.2	6.43	0.69	6.44	1.30	8.55	1.90	5.75	0.87	5.14	0.72	130	30.7	0.33	3.50
	6914	10.56	9.97	23.6	3.02	11.0	2.56	0.31	2.39	0.43	2.23	0.40	0.95	0.14	0.79	0.13	50.5	7.46	0.39	8.40
	6972	6.66	3.37	7.57	0.70	3.42	0.82	0.25	0.91	0.07	1.15	0.11	0.58	0.01	0.47	0.01	16.1	3.32	0.89	4.81
DD	**7742**	23.67	29.61	60.1	8.25	33.9	7.10	2.01	6.74	1.04	5.36	1.03	2.58	0.36	2.08	0.33	141	19.5	0.89	9.51
FD	**6589**	39.40	5.49	8.28	0.73	2.38	0.51	0.72	0.94	0.37	4.41	1.55	6.47	1.24	8.48	1.22	18.1	24.7	3.19	0.43
	7733	18.28	9.57	24.0	2.65	9.82	2.56	0.28	2.40	0.56	3.44	0.67	2.08	0.35	2.54	0.40	48.9	12.4	0.34	2.52
EqG	**7233**	12.74	11.41	28.70	3.04	14.0	3.23	0.24	2.98	0.43	2.92	0.39	1.21	0.05	1.02	0.03	60.7	9.03	0.24	7.52
	7400	14.33	18.79	42.41	4.77	21.8	4.79	0.41	4.07	0.51	3.21	0.41	1.30	0.05	1.06	0.03	92.9	10.6	0.29	11.7

nd: not determinated; *data from Sardi *et al*. (2010); [a]data from Grosse *et al*. (2009).
**data only Y from Sardi *et al*. (2010).
Major elements in wt% and trace elements in ppm. ACNK Alumina saturation index.

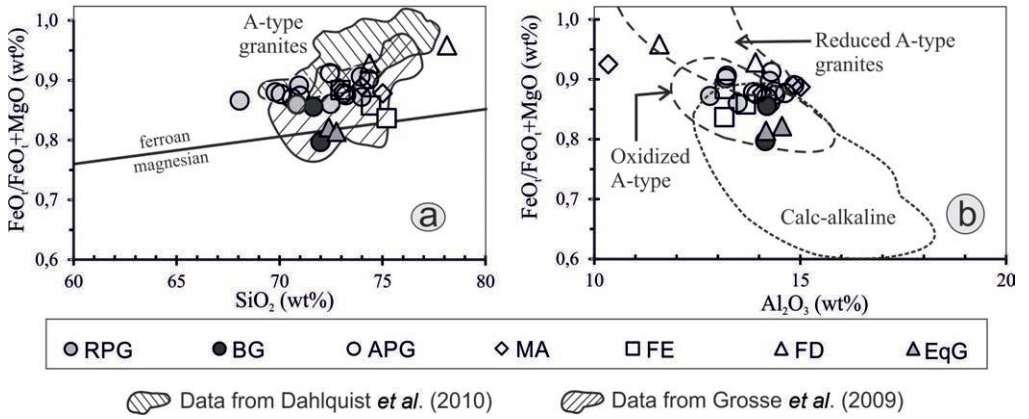

FIG. 6. Geochemical diagrams. **a.** FeO_t/FeO_t+MgO (wt%) *versus* SiO_2 (wt%) with A-type granites field of Frost *et al*. (2001). Data of previous works on the Huaco Granite Pluton and other typical A-type granites from the Velasco range and surrounding areas are included in the diagram (Grosse *et al*., 2009; Dahlquist *et al*., 2010). **b.** FeO_t/FeO_t+MgO (wt%) *versus* Al_2O_3 (wt%) indicating the field of oxidized and reduced A-type granites of Dall'Agnol and Oliveira (2007).

in agreement with Grosse *et al*. (2009) and Dahlquist *et al*. (2010). In the diagram of Dall' Agnol and Oliveira (2007) (Fig. 6b) the samples plot in both the "reduced" and "oxidized" A-type granite fields.

Regarding trace element contents, the rocks show both differences and similarities. In the case of Cs, the lowest values are in samples of the FD and FE (~4 and ~12 ppm, respectively), and the highest ones in samples of the EqG and APG (~115 ppm). Lower Rb contents (<300 ppm) are recorded in the BG facies and in one sample of the FD, while the highest content corresponds to a sample of the APG (658 ppm). Roughly, Ba and Sr contents gradually increase in the following sequence: MA, FD, FE, EqG, APG, RGP, BG. The BG facies contains the lowest Rb/Sr (3.6 and 3.8) and highest Ba/Rb (0.95 and 1.27) ratios, whereas the MA contains the highest (17.4-47.0) and lowest (0.09-0.19) ratios, respectively.

Finally, the La Chinchilla stock is very rich in SiO_2, weakly peraluminous, has very low Ca, P, Fe and Mg contents, and is strongly enriched in several trace elements, particularly Li, Rb, Nb, Ta, U, Th, Y and HREE (Grosse *et al*., 2009). Grosse *et al*. (2009), based on Nd isotopes, suggest that the La Chinchilla stock derived from a different, more primitive source compared to the Huaco granite; we do not consider it further in this study.

ME and DD: The 6 analyzed mafic enclaves have variable compositions that can be attributed to different degrees of assimilation and hybridization with the host rock. Three samples have low SiO_2 contents (<57%) and can be considered slightly assimilated by the granite magma, whereas one of them contains 70% SiO_2, similar to the host granite.

The ME samples have very high concentrations in FeOt and MgO and their abundances are inversely proportional to the SiO_2 content. They are also rich in CaO and P_2O_5. The alkali contents do not vary with SiO_2. The FeO_t/FeO_t+MgO ratios in the ME are variable between 0.69 and 0.86.

The dioritic dike (DD) shows evidence of assimilation of felsic material. The analyzed sample has a low SiO_2 content (56.6%), similar to the less assimilated mafic enclaves. It presents high contents of ferromagnesian elements, CaO, alkalis and P_2O_5. Compared to the less assimilated mafic enclaves, it is poor in FeO_t and rich in MgO, so its FeO_t/FeO_t+MgO ratio is very low (0.68). The ASI of the DD is 0.84. On the other hand, the DD has a composition that is very similar to mafic dikes hosted in the Carboniferous San Blas granite in the north of the Velasco range (Báez, 2006).

The Cs (37-175 ppm), Rb (220-2758 ppm), Ba (118-189 ppm) and Sr (26-121 ppm) contents in the mafic enclaves (ME) are variable, whereas the DD has values of 28 ppm, 131 ppm, 222 ppm and 477 ppm, respectively.

4.2.2. REE and Y composition

Y content is greater in the RPG and APG than in all other granitoid rocks, but the values of Y in the mafic enclaves (ME) are similar to the RPG.

LREE>HREE is observed in all facies of Huaco granite and associated rocks, with the exception of the garnet-bearing felsic dike (sample 6589). The highest REE contents (>170 ppm) are found in the RPG, BG, APG and ME (Table 1, Fig. 7). The RPG, BG and APG show similar chondrite-normalized REE patterns and La_n/Yb_n ratios always >5. The EqG have lower REE contents but similar La_n/Yb_n ratios also >5 (Table 1, Fig. 7). The FE, MA and FD have the lowest concentrations of REE and the lowest La_n/Yb_n ratios, mostly <5 (Table 1, Fig. 7). The Eu/Eu* ratio is <1 and the La_n/Yb_n ratio is >1 for all rocks, with the exception of the FD garnet-bearing sample (Table 1 and Fig. 7).

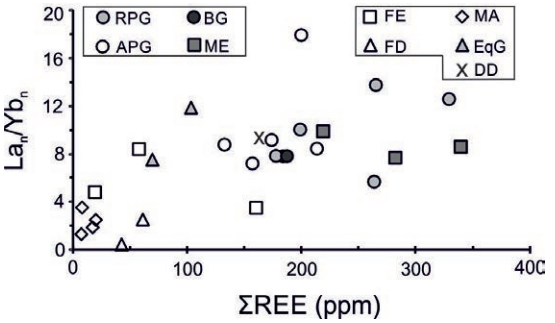

FIG. 7. La_n/Yb_n* *versus* ΣREE orthogonal diagram. *Normalized after Nakamura (1974).

5. Discussion

Based on Nd and Sr isotopic data (εNd -2.10 to -4.27; Sr^{87}/Sr^{86} 0.7820 to 0.8825) and geochemical features such as high and restricted SiO_2 contents, peraluminous character, high contents of LIL and other trace elements such Nb, Y and Ga, Grosse *et al*. (2009) and Dahlquist *et al*. (2010) suggested that the Huaco pluton, as a whole, formed from a mainly crustal source (possibly the Ordovician meta-granites), with minor participation of a mantle-derived component, and intruded in a dominantly extensional setting. The study of each minor facies and associated igneous rocks can give further clues on the evolution of the granite pluton.

Both the BG and the APG are coeval with the RPG. The BG possibly formed on the walls of the magmatic chamber, whereas the APG formed around the BeP. A temporal sequence of crystallization in the order BG → RPG → APG is favored by the slight decrease in the biotite/muscovite ratio and by their LIL contents (see below). The finer-grained texture of the BG and APG facies compared to the RPG facies suggests faster growth rates for the BG and APG during slightly lower temperature conditions (*e.g.,* Vernon, 1986).

Figures 8a and b present major and trace element variation diagrams with SiO_2 (wt%) as a differentiation index for the facies and associated rocks of granitic composition. Although samples of the RPG, BG and APG are fairly scattered in the diagrams, they show rough trends. These trends are better defined for TiO_2, Al_2O_3, ferromagnesian elements, CaO, Ba and Sr, and weakly marked for Na_2O, K_2O, Cs, Rb, Ba/Rb and REE. Y shows a sub-horizontal tendency and the Rb/Sr ratio a slightly positive tendency. These trends suggest a fractional crystallization process for the RPG, BG and APG, as previously indicated by Sardi *et al*. (2010, 2011). The remaining rocks appear to be unrelated to these trends, particularly in the cases of TiO_2, the ferromagnesian elements, Ba and Sr.

Large-ion lithophile elements such as Rb, Sr, Ba and Cs and their ratios, as well as the REE, are commonly used as monitors of magmatic differentiation (*e.g.,* Halliday *et al*., 1991; Morteani *et al*., 1995; Icenhower and London, 1996; Nabelek and Bartlett, 1998; Nabelek, 1999; Jung *et al*., 2000; Dahlquist *et al*., 2007). Therefore, we have applied a fractional crystallization model to investigate the behavior of Rb, Sr, Ba and also the REE during this process in the Huaco granite pluton. The used equation is the well-known Rayleigh fractionation: $C_l/C_o=f^{(D-1)}$ (taken from Rollinson, 1998), where C_l is the weight concentration of a trace element in the magmatic liquid; C_o is the weight concentration in the parental liquid, which we consider it to be the BG facies; *f* is the fraction of melt remaining; and D is the bulk distribution coefficient of the fractionating assemblage during crystal fractionation. The different values of Kd coefficients were taken from Arth (1976), Rapela and Shaw (1979), Nash and Crecraft (1985) and Icenhower and London (1996).

According to the obtained values of D ($D_{Sr, Ba}$ >1 and D_{Rb}<1; Rollinson, 1998), Sr and Ba are considered "compatible elements" and Rb as "incompatible" element. The evolutionary models were calculated assuming a starting melt with 285.9 ppm Rb, 318.5 ppm Ba and 77.5 ppm Sr, which are the average values of the two BG samples. The average values

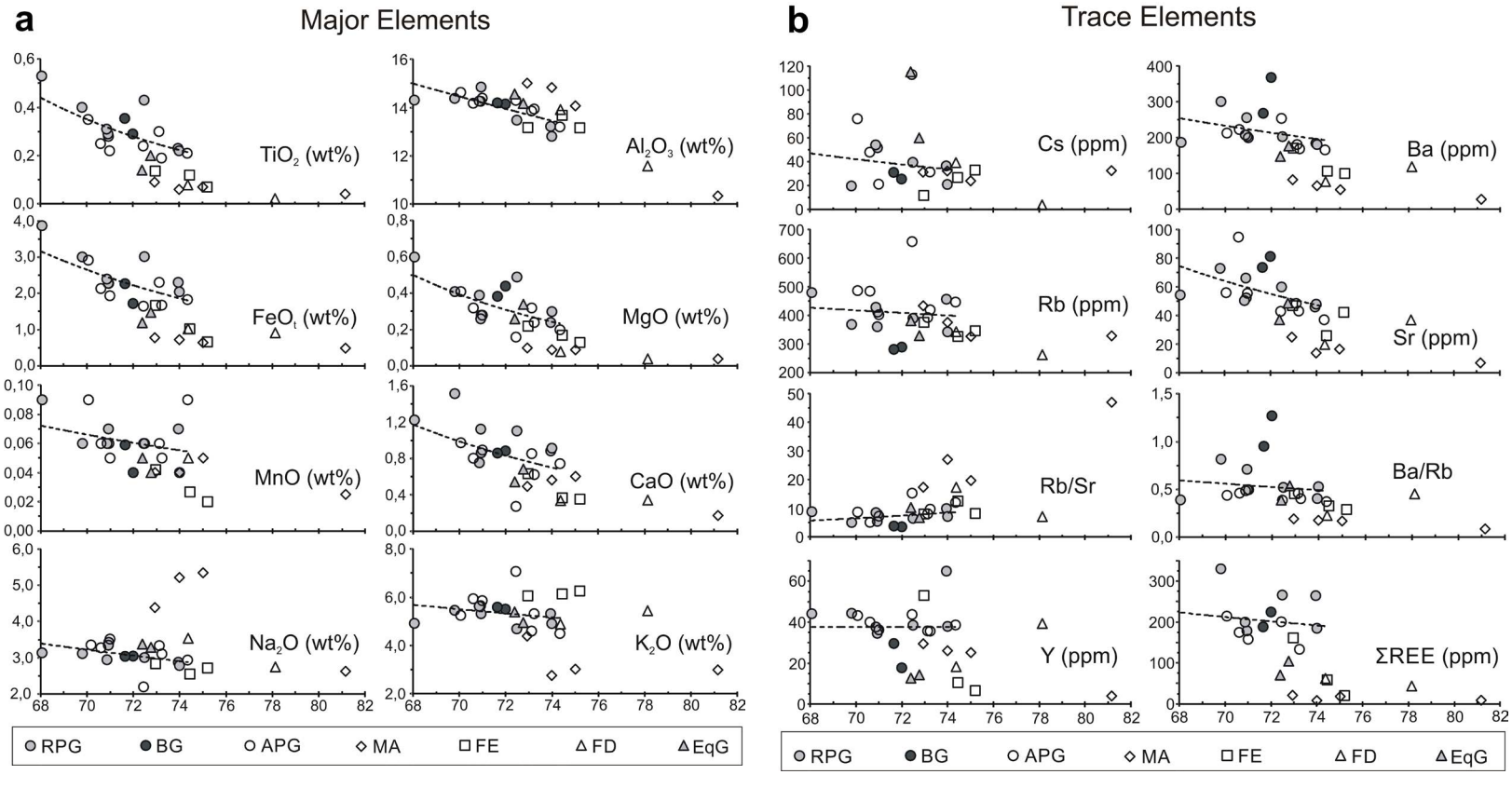

FIG. 8. "Harker" diagrams, with SiO_2 (wt%) as indicator of differentiation ("x axis") (Only "granitoid" facies and rocks are considered). Variation line is calibrated by least square regressions considering the main and coeval facies (RPG, BG and APG). **a.** Major elements; **b.** Trace elements.

of the BG samples were also used for the REE. The mode of fractionating minerals is also an average value of these samples: 37% quartz, 26% K-feldspar; 29% plagioclase; 5% biotite and 3% muscovite.

Figure 9 show the hypothetical Rb, Sr and Ba compositions in the calculated liquid according to the Rayleigh fractionation model. Comparison between the theoretical compositions and the samples show a correlation for the BG, RPG and APG, whereas the MA, ME, FE, DD, FD and EqG plot away from the theoretical curves, mostly below them. Therefore, we propose that the coeval RPG, BG and APG facies are related to each other by a fractional crystallization process, whereas the other facies and associated rocks were not involved in this process. The REE compositions also show correlation with the fractional crystallization model for the coeval RPG-BG-APG facies, which furthermore have a notable parallelism in the normalized-diagrams (Fig. 10a). Probably due to high contents of REE-fractionated minerals (*e.g.,* biotite), the ME plot close to the theoretical model, but we cannot suggest any relation with the main facies by means of this process, at least given the geochemical data (Fig. 10b). The other facies and associated rocks seem to have no relationship with the fractional crystallization model (Fig. 10a, b, and c).

Given their mostly ellipsoidal shapes and the presence of the APG surrounding them, the BeP probably formed when the main RPG was not fully crystallized. Hence, the BeP can be considered coeval to the final stage of the RPG, rather than an independent event. This also applies to the OG (Grosse *et al*., 2010). The internal structure of the BeP indicates a progressive sequence of crystallization from the aplitic margins (the MA) towards the interior of the intra-granitic pegmatitic cavity (*e.g.,* Cameron *et al*., 1949; Černý, 1991; Stilling *et al*., 1996). The BeP and the OG point to the importance of water and/or volatiles in the late stages of crystallization of the main granite. The formation of the BeP and its main accessory mineral, beryl, require conditions of water-saturation and the presence of volatiles (Jahns and Burnham, 1969; Evensen *et al*., 1999). The circulation of water during pegmatitic crystallization is also manifested by the Na-metasomatism present in the pegmatite bodies (Sardi *et al*., 2015).

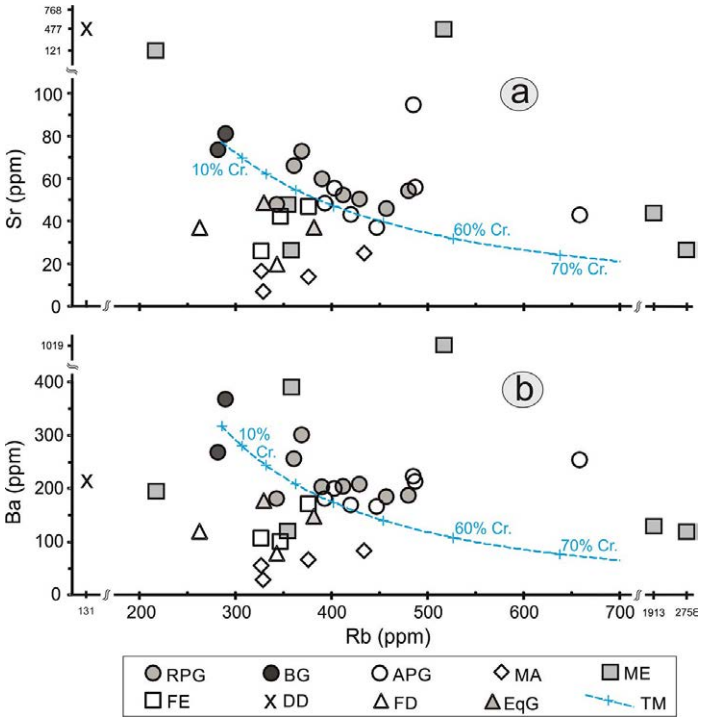

FIG. 9. Sr-Rb **(a)** and Ba-Rb **(b)** diagrams showing measured contents and theoretical concentrations obtained from the crystal fractionation model. **Cr.:** crystallization; **TM:** theoretical model.

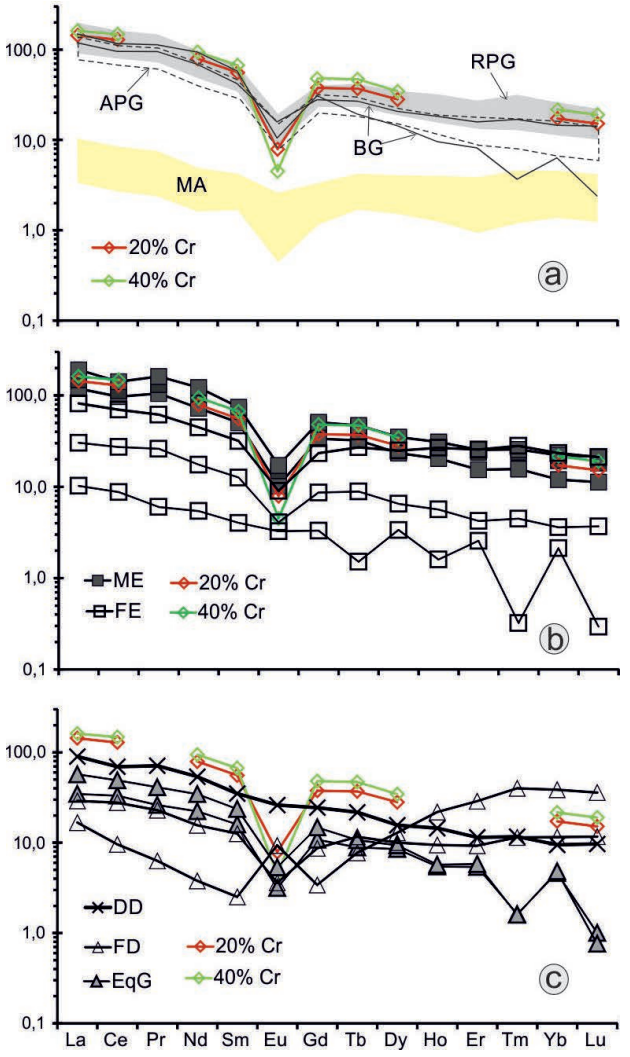

FIG. 10. Chondrite-normalized REE patterns of the different facies of the Huaco granite pluton and associated rocks. **a.** Main and coeval (to-late) facies: RPG, BG, APG and MA; **b.** Enclaves: ME and FE; **c.** Dikes (DD and FD) and Equigranular Granites (EqG). Normalization values after Nakamura (1974). In color calculated patterns, in red 20% crystallization, in green 40% crystallization.

Likewise, high water content and its exsolution probably was the driving force for the fomation of the OG (Grosse *et al*., 2010).

The presence of monazite and other accessory minerals such as apatite can play an important role in LREE fractionation (*e.g.,* Broska *et al*., 2000; Dahlquist, 2001). Apparently, the behavior of the HREE could have been controlled by the presence of garnet rather than monazite (Duke *et al*., 1992), as is clearly observed in one sample of the FD. The MA, FE and FD facies with values of La_n/Yb_n generally less than 6, could have formed at a lower temperature than the main regional facies (RPG). The negative Eu anomaly (Eu/Eu* <1) observed in several facies and associated rocks of the Huaco granite pluton can be attributed to the fractionation of feldspars. However, the unique positive Eu anomaly observed in one sample of the FD is attributed to garnet as accessory mineral (Fig. 10c) (*e.g.,* Henderson, 1984).

Features shown by the ME suggest that they are mafic magma globules incorporated into the host

granite, *i.e*., rounded or oval shapes, cooling edges, fine to very fine grained texture, incorporation of host magma megacrysts and presence of acicular apatite, indicative of fast cooling and mingling (*e.g.,* Michel *et al*., 2016). In addition, the ME have higher εNd values (-0.55 and 0.61; Grosse *et al*., 2009) than the host granite ($\varepsilon Nd_{\text{Huaco Granite (RPG facies)}}$ -4.27 to -2.10; Grosse *et al*., 2009), suggesting a more primitive source. On the other hand, the ME have high initial $^{87}Sr/^{86}Sr$ ratios (0.8586 and 0.8680, Grosse *et al*., 2009). This decoupling behavior of Sr and Nd isotopes is common in enclaves of this type (*e.g.,* Holden *et al*., 1991; Lesher, 1990 and 1994; Pin *et al*., 1990; Allen, 1991). Hence, the ME may be considered primitive remnants of the mafic component of the pluton.

The FE can be considered "premature" aplites that formed when partially crystallized granitic magma "breaks" along planes allowing the intrusion of aplites, which are then dismembered due to the movement of the magma. Alternatively, the FE could have been part of a first pulse of felsic magma that crystallized at the margins of the magma chamber and was later dismantled and incorporated by the main granitic magmas. Remnants of these felsic margins could be the felsic facies described by Rossi *et al*. (2005b) at the eastern border of the Huaco granite pluton.

The occurrence of the DD suggests that they may correspond to an independent/unrelated and younger episode, since this type of dioritic dikes, cutting felsic igneous bodies, is common in extensional post-orogenic settings (*e.g.,* Hegner *et al*., 1998).

The EqG are temporally younger than the main facies as they contain enclaves of the RPG. Grosse (2007) had suggested that the EqG originated from a purely crustal source and therefore are not final melts of the RPG. A purely crustal source is in agreement with the lack of tonalitic enclaves in the EqG and their chemical compositions similar to experimental melts derived from crustal rocks (*e.g.,* the peraluminous orthogneisses of Holtz and Johannes, 1991; Grosse, 2007).

6. Conclusions

The Huaco granite pluton (Velasco Range, northwest Argentina) is composed by one main facies (RPG) and two subordinate facies that are coeval and co-genetic (BG and APG), as well as two coeval-to-late co-genetic facies (BeP and OG). In addition, it is host to temporally previous (ME and FE) and posterior (FD, DD and EqG) associated rocks.

Based on field observations, petrography, LIL and REE compositions, the main and coeval facies formed by fractional crystallization from the main magma in the sequence BG-RPG-APG, from the wall towards the interior of the chamber and finally around the Be-pegmatites.

The other units had distinct magmatic evolutions: **i)** the ME are partially assimilated remnants of mafic, mantle-derived components; **ii)** the FE are remnants of premature aplites or of an initial felsic pulse; **iii)** the BeP, FD and OG are related to abundant contents of water and/or volatiles and formed during the final stage of crystallization of the main granitic facies (BeP and OG) or after it (FD); **iv)** the EqG intruded the RPG and seem to have a purely crustal source, suggesting a second batch of fusion without a mafic component (with the exception of the La Chinchilla stock, which has features suggesting a more primitive source); and **v)** the DD are possibly associated to a younger episode of mafic, mantle-derived magmatism related to extension, although gechemical data is needed to better constrain its origin.

Acknowledgements

Funding for this project was provided by the following organizations: Consejo Nacional de Investigaciones Científicas y Tecnológicas (CONICET, Argentina), Naruto University of Education, Department of Geosciences (Japan) and Museo Geominero (Instituto Geológico y Minero de España. We thank the reviewers which helped improve the quality of this article. Also, we thank Dr. W. Vivallo for his editorial handling of the manuscript.

References

Abdel Rahman, A. 1994. Nature of biotite from alkaline, calc-alkaline, and peraluminous magmas. Journal of Petrology 35: 525-541.

Alasino, P.; Dahlquist, J.; Pankhurst, R.; Galindo, C.; Casquet, C.; Rapela, C.; Larrovere, M.; Fanning, C. 2012. Early Carboniferous sub- to mid-alkaline magmatism in the Eastern Sierras Pampeanas, NW Argentina: A record of crustal growth by the incorporation of mantle-derived material in an extensional setting. Gondwana Research 22: 992-1008.

Allen, C. 1991. Local equilibrium of mafic enclaves and granitoids of the Turtle Pluton, southeast California:

mineral, chemical and isotopic evidence. American Mineralogist 76: 574-588.

Arth, J. 1976. Behaviour of trace elements during magmatic processes -a summary of theroretical models and their applications. Journal of Research of the U.S. Geological Survey 4: 41-47.

Báez, M. 2006. Geología, petrología y geoquímica del basamento ígneo-metamórfico del sector norte de la sierra de Velasco, provincia de La Rioja. Ph.D. Thesis (Unpublished), Universidad Nacional de Córdoba: 207 p.

Báez, M.; Bellos, L.; Grosse, P.; Sardi, F. 2005.Caracterización petrológica de la sierra de Velasco. *In* Geología de la provincia La Rioja (precámbrico-paleozoico inferior) (Dalhquist, J.; Baldo, E.; Alasino, P.; editors). Asociación Geológica Argentina, Serie D: Publicación especial No.8: 123-130.

Bellos, L. 2005. Geología y petrología del sector austral de la Sierra de Velasco, al sur de los 29º44' S, La Rioja, Argentina. Serie de Correlación Geológica 19: 261-278.

Bellos, L.; Castro, A.; Díaz-Alvarado, J.; Toselli, A. 2015. Multi-pulse cotectic evolution and in-situ fractionation of calc-alkaline tonalite-granodiorite rocks, Sierra de Velasco batholith, Famatinian belt, Argentina. Gondwana Research 27 (1): 258-280.

Breiter, K.; Müller, A.; Leichmann, J.; Gabašová, A. 2005. Textural and chemical evolution of a fractionated granitic system: the Podlesí stock, Czech Republic. Lithos 80: 323-345.

Broska, I.; Petrík, I.; Williams, T. 2000. Coexisting monazite and allanite in peraluminous granitoids of the Tribeč Mountains. Western Carpathians American Mineralogist 85: 22-32.

Cameron, E.; Jahns, R.; McNair, A.; Page, L. 1949. Internal structure of granitic pegmatites. Economic Geology, Monographs 2: 115.

Černý, P. 1991. Rare-element granitic pegmatites. Part I: anatomy and internal evolution of pegmatite deposits and Part II: regional to global environments and petrogenesis. Geoscience Canada 18 (2): 49-81.

Černý, P.; Masau, M.; Goad, B.; Ferreira, K. 2005. The Greer Lake leucogranite, Manitoba, and the origin of lepidolite-subtype granitic pegmatites. Lithos 80: 305-321.

Collins, W.; Beams, S.; White, A.; Chappell, B. 1982. Nature and origin of A-type granites with particular reference to southeastern Australia. Contrib Mineral Petrol 80: 189-200.

Cravero, O. 2005. Las pegmatitas zonadas de la sierra de Velasco, La Rioja. Serie de Correlación Geológica 19: 133-144.

Dahlquist, J. 2001. REE fractionation by accessory minerals in epidote-bearing metaluminous granitoids from the Sierras Pampeanas, Argentina. Mineralogical Magazine 65 (4): 463-475.

Dahlquist, J.; Pankhurst, R.; Rapela, C.; Casquet, C.; Fanning, C.; Alasino, P.; Báez, M. 2006. The San Blas Pluton: An example of Carboniferous plutonism in the Sierras Pampeanas, Argentina. Journal of South American Earth Sciences 20: 341-350.

Dahlquist, J.; Galindo, C.; Pankhurst, R.; Rapela, C.; Alasino, P.; Saavedra, J.; Fanning, C. 2007. Magmatic evolution of the Peñon Rosado granite: Petrogenesis of garnet-bearing granitoids. Lithos 95: 177-207.

Dahlquist, J.; Alasino, P.; Eby, N.; Galindo, C.; Casquet, C. 2010. Fault controlled Carboniferous A-type magmatism in the proto-Andean foreland (Sierras Pampeanas, Argentina): Geochemical Constraints and Petrogenesis. Lithos 115: 65-81.

Dahlquist, J.; Pankhurst, R.; Gaschnig, R.; Rapela, C.; Casquet, C.; Alasino, P.; Galindo, C.; Baldo, E. 2013. Hf and Nd isotopes in Early Ordovician to Early Carboniferous granites as monitors of crustal growth in the Proto-Andean margin of Gondwana. Gondwana Research 23: 1617-1630.

Dall'Agnol, R.; Oliveira, D. 2007. Oxidized, magnetite-series, rapakivi-type granites of Carajás, Brazil: Implications for classification and petrogenesis of A-type granites. Lithos 93: 215-233.

De Los Hoyos, C.; Willner, A.; Larrovere, M.; Rossi, J.; Toselli, A.; Basei, M. 2011. Tectonothermal evolution and exhumation history of the Paleozoic Proto-Andean Gondwana margin crust: The Famatinian Belt in NW Argentina. Gondwana Research 20: 309-324.

Duke, E.; Papike, J.; Laul, J. 1992. Geochemistry of a boron-rich peraluminous granite pluton: The Calamity Peak Layered granite-pegmatite complex, Black Hill, South Dakota. Canadian Mineralogist 30: 811-833.

Eby, G. 1990. The A-type granitoids: a review of their occurrence and chemical characteristics and speculations on their petrogenesis. Lithos 26:115-134.

Eby, G. 1992. Chemical subdivision of the A-type granitoids: petrogenetic and tectonic implications. Geology 20: 641-644.

Evensen, J.; London, D.; Wendlandt, R. 1999. Solubility and stability of beryl in granitic melts. American Mineralogist 84: 733-745.

Frost, B.; Barnes, C.; Collins, W.; Arculus, R.; Ellis, D.; Frost, C. 2001. A geochemical classification for granitic rocks. Journal of Petrology 42: 2033-2048.

González Bonorino, F. 1951. Una nueva formación Precámbrica en el noroeste Argentino. Comunicación Científica, Museo de La Plata 5: 4-6.

Grosse, P. 2007. Los granitos porfíricos y orbiculares del sector Centro-Oriental de la Sierra de Velasco. Génesis y significación regional. Provincia de la Rioja. R. Argentina (Unpublished) Ph.D. Thesis, Universidad Nacional de Córdoba: 285 p.

Grosse, P.; Sardi, F. 2005. Geología de los granitos Huaco y Sanagasta, sector centro-oriental de la Sierra de Velasco, La Rioja. Serie de Correlación Geológica 19: 221-238.

Grosse, P.; Bellos, L.; Báez, M.; Rossi, J.; Toselli, A. 2003. Ordovician magmatism of the Sierra de Velasco, La Rioja, Argentina. Serie de Correlación Geológica 17: 223-226.

Grosse, P.; Larrovere, M.; De la Rosa, J.D.; Castro, A. 2005. Petrología y origen del stock La Chinchilla, Sierra de Velasco, La Rioja (Argentina). *In* Congreso Geológico Argentino, No. 16, Acta 1: 533-538. Buenos Aires.

Grosse, P.; Rossi, J.N.; Sardi, F.; Toselli, A. 2006. Química mineral de los granitos Sanagasta, Huaco y La Chinchilla, Sierra de Velasco, La Rioja, Argentina. *In* Congreso de Mineralogía y Metalogenia, No. 8, Actas: 381-388. Buenos Aires.

Grosse, P.; Söllner, F.; Báez, M.; Toselli, A.; Rossi, J.; De la Rosa, D. 2009. Lower Carboniferous post-orogenic granites in central-eastern Sierra de Velasco, Sierras Pampeanas, Argentina: U-Pb monazite geochronology, geochemistry and Sr-Nd isotopes. The International Journal of Earth Sciences 98: 1001-1025.

Grosse, P.; Toselli, A.; Rossi, J. 2010. Petrology and geochemistry of the orbicular granitoid of Sierra de Velasco (NW Argentina) and implications for the origin of orbicular rocks. Geological Magazine 147: 451-468.

Grosse, P.; Bellos, L.; De Los Hoyos, C.; Larrovere, M.; Rossi, J.; Toselli, A. 2011. Across-arc variation of the Famatinian magmatic arc (NW Argentina) exemplified by I-, S- and transitional I/S-type Early Ordovician granitoids of the Sierra de Velasco. Journal of South American Earth Sciences 32: 110-126.

Halliday, A.; Davidson, J.; Hildreth, W.; Holden, P. 1991. Modelling the petrogenesis of high Rb/Sr silicic magmas. Chemical Geology 92: 107-114.

Hegner, E.; Kölbl-Ebert, M.; Loeschke, J. 1998. Post-collisional Variscan lamprophyres (Black Forest, Germany): $^{40}Ar/^{39}Ar$ phlogopite dating, Nd, Pb, Sr isotope and trace elements characteristics. Lithos 45: 395-411.

Henderson, P. 1984. Rare Earth Elements Geochemistry. Elsevier: 510 p.

Höckenreimer, M.; Söllner, F.; Miller, H. 2003. Dating the TIPA shear zone: Early Devonian terrane boundary between Famatinian and Pampean systems (NW Argentina). Journal of South American Earth Sciences 16 (1): 45-66.

Holden, P.; Halliday, A.; Stephens, W.; Henney, P. 1991. Chemical and isotopic evidence for major mass transfer between mafic enclaves and felsic magma. Chemical Geology 92: 135-152.

Holtz, F.; Johannes, W. 1991. Genesis of peraluminous granites I. Experimental investigation of melt compositions at 3 and 5 kb and various H_2O activities. Journal of Petrology 32: 935-958.

Icenhower, J.; London, D. 1996. Experimental partitioning of Rb, Cs, Sr, and Ba between alkali feldspar and peraluminous melt. American Mineralogist 81: 719-734.

Jahns, R.; Burnham, C. 1969. Experimental studies of pegmatite genesis: I. A model for the derivation and crystallization of granitic pegmatites. Economic Geology 64: 843-864.

Jung, S.; Hoernes, S.; Mezger, K. 2000. Geochronology and petrogenesis of Pan-African, syn-tectonic, S-type and post-tectonic A-type granite (Namibia): products of melting of crustal sources, fractional crystallization and wall rock entrainment. Lithos 50: 259-287.

Larrovere, M.; De Los Hoyos, C.; Toselli, A.; Rossi, J.; Basei, M.; Belmar, M. 2011. High T/P evolution and metamorphic ages of the migmatitic basement of northern Sierras Pampeanas, Argentina: Characterization of a mid-crustal segment of the Famatinian belt. Journal of South American Earth Sciences 31: 279-297.

Larrovere, M.; De Los Hoyos, C.; Grosse, P. 2012. Los complejos metamórficos del retro-arco Famatiniano (noroeste de Argentina): caracterización geoquímica e isotópica de sus protolitos e implicancias geotectónicas. Revista Mexicana de Ciencias Geológicas 29 (3): 676-695.

Lesher, C. 1990. Decoupling of chemical and isotopic exchange during magma mixing. Nature 344: 235-237.

Lesher, C. 1994. Kinetics of Sr and Nd exchange in silicate liquids: theory, experiments, and applications to uphill diffusion, isotopic equilibration, and irreversible mixing magma. Journal of Geophysical Research 99: 9585-9604.

Macchioli Grande, M.; Alasino, P.H.; Rocher, S.; Larrovere, M.A.; Dahlquist, J.A. 2015. Asymmetric textural and structural patterns of a granitic body emplaced at shallow levels: The La Chinchilla pluton, northwestern

Argentina. Journal of South American Earth Sciences 64: 58-68.

Michel, L.; Wenzel, T.; Markl, G. 2016. Interaction between two contrasting magmas in the Albtal pluton (Schwarzwald, SW Germany): textural and mineral-chemical evidence. International Journal of Earth Science 5: 1505-1524.

Morello, O.; Aparicio González, P. 2013. Mineralización de uranio en la sierra de Velasco, La Rioja. Revista de la Asociación Geológica Argentina 70 (3): 335-340.

Morteani, G.; Preinfalk, C.; Spiegel, W.; Bonalumi, A. 1995. The Achala Granitic Complex and the Pegmatites of the Sierras Pampeanas (Northwest Argentina): A study of differentiation. Economic Geology 90: 636-647.

Muñoz, J. 1984. F-OH and Cl-OH exchange in micas with applications to hydrothermal ore deposits. *In* Reviews in Mineralogy, Micas (Bailey, S.; editors). Mineralogical Society of America 13: 469-493.

Nakamura, N. 1974. Determination of REE, Ba, Mg, Na and K in carbonaceous and ordinary chondrites. Geochimica et Cosmochimica Acta 38: 757-773.

Nash, W.; Crecraft, H. 1985. Partition coefficients for trace elements in silicic magmas. Geochimica et Cosmochimica Acta 49: 2309-2322.

Nabelek, P. 1999. Trace element distribution among rock-forming minerals in Black Hills migmatites,South Dakota: A case for solid-state equilibrium. American Mineralogist 84: 1256-1269.

Nabelek, P.; Bartlett, C. 1998. Petrologic and geochemical links between the post-collisional Proterozoic Harney Peak leucogranite, South Dakota, USA, and its source rocks. Lithos 45: 71-85.

Pankhurst, R.J.; Rapela, C.; Saavedra, J.; Baldo, E.G.; Dahlquist, J.; Pascua, I.; Fanning, C.M. 1998. The Famatinian arc in the central Sierras Pampeanas: an early to mid-Ordovician continental arc on the Gondwana margin. *In* The Proto-Andean Margin of Gondwana (Pankhurst, R.J.; Rapela, C.; editors). Geological Society of London, Special Publication 142: 343-367.

Pankhurst, R.J.; Rapela, C.; Fanning, C. 2000. Age and origin of coeval TTG, I- and S- type granites in the Famatinian belt of NW Argentina. Transactions of the Royal Society of Edinburgh: Earth Sciences 91: 151-168.

Parra, F.; Blason, R.; Álvarez, J.; Zarco Ambrosio, J.; Bello, C. 2011. Estimación de recursos uraníferos en el Stock La Chinchilla, sierra de Velasco, provincia de La Rioja. *In* Congreso Geológico Argentino, No. 18, Proceeding: CD-Room (2 pages).

Pin, C.; Binon, M.; Belin, J.; Barbarin, B.; Clemens, J. 1990. Origin of microgranular enclaves in granitoids: equivocal Sr-Nd evidence from Hercynian rocks in the Massif Central (France). Journal of Geophysical Research 95: 17821-17828.

Quartino, B.; Villar Fabre, J. 1962. El cuerpo granítico orbicular precámbrico de la Pampa de Los Altos, sierra de Velasco. Revista de la Asociación Geológica Argentina 18: 11-41.

Rapela, C.; Shaw, D. 1979. Trace and major element models of granitoid genesis in the Pampean Ranges, Argentina. Geochimica et Cosmochimica Acta 43: 1117-1129.

Rapela, C.; Casquet, C.; Baldo, E.; Dahlquist, J.; Pankhurst, R.; Galindo, C.; Saavedra, J. 2001. Las Orogénesis del Paleozoico Inferior en el margen proto-andino de América del Sur, Sierras Pampeanas, Argentina. Journal of Iberian Geology 27: 23-41.

Rollinson, H. 1998. Using geochemical data: evaluation, presentation, interpretation. Longman: p. 352.

Rossi, J.; Willner, A.; Toselli, A. 2002. Ordovician Metamorphism of the Sierras Pampeanas, Sistema de Famatina and Cordillera Oriental, Northwestern Argentina. Serie de Correlación Geológica 16: 225-242.

Rossi, J.; Toselli, A.; Báez, M. 2005a. Evolución termobárica del ortogneis peraluminoso del noroeste de la sierra de Velasco, La Rioja. Asociación Geológica Argentina, Revista 60: 278-289.

Rossi, J.; Toselli, A.; Prieri, A.; Cravero, O.; De Los Hoyos, C. 2005b. Granitos cordieríticos y corneanas del flanco oriental de la sierra de Velasco, La Rioja, República Argentina. *In* Congreso Geológico Argentino, No. 16, Proceedings: CD-Room (4 pages).

Salvatore, M.; Parra, F.; Sánchez, D.; Álvarez, J.; Bello, C.; Zarco Ambrosio, J. 2011. Mapeo detallado de facies graníticas en el Stock uranífero La Chinchilla, sierra de Velasco, provincia de La Rioja. *In* Congreso Geológico Argentino, No. 18, Proceeding CD-Room: 2 p.

Salvatore, M.; Parra, F.; Sánchez, D.; Álvarez, J.; Bello, C.; Zarco Ambrosio, J. 2013. Caracterización litogeoquímica del granito La Chinchilla y su relación con el uranio, sierra de Velasco, Provincia de La Rioja. Revista de la Asociación Geológica Argentina 70 (3): 341-350.

Sardi, F.; Toselli, A.; Rossi de Toselli, J.N. 2002. Estudio geológico preliminar de las pegmatitas del Norte del Bolsón de Huaco, sierra de Velasco, La Rioja. *In* Congreso Geológico Argentino, No. 15 (Cabaleri, N.; Cingolani, C.; Linares, E.; López de Luchi, M.; Ostera, H.; Panarello, H.; editors). Actas 2: 33-34. El Calafate.

Sardi, F.; Murata, M.; Grosse, P. 2010. Petrographical and geochemical features of the granite-pegmatite transition in the Velasco Pegmatitic District, NW Argentina. Neues Jahrbuch für Geologie und Paläontologie 258: 61-71.

Sardi, F.; Murata, M.; Grosse, P. 2011. Magmatic differentiation in the Huaco granite and its associated Be-pegmatites from the Velasco district, Argentina. *In* International Symposium on Granitic Pegmatites, No. 5, Abstract book: 189-191. Mendoza.

Sardi, F.G.; Heimann, A.; Sarapura Martínez, J. 2015. Geología local y mineralogía accesoria de las pegmatitas berilíferas del Distrito Velasco y rocas graníticas asociadas, Provincia Pegmatítica Pampeana, Noroeste de Argentina. Serie de Correlación Geológica 31 (1): 111-132.

Smith, D.; Noblett, J.; Wobus, R.; Unruh, D.; Douglass, J.; Beance, R.; Davis, C.; Goldman, S.; Kay, G.; Gustavson, B.; Saltoun, B.; Stewart, J. 1999. Petrology and geochemistry of late-stage intrusions of the A-type, mid-Proterozoic Pikes Peak batholith (Central Colorado, USA): implications for petrogenetic models. Precambrian Research 98: 271-305.

Stilling, A.; Černý, P.; Vanstone, P. 2006. The Tanco pegmatite at Bernic Lake, Manitoba. XVI. Zonal and bulk compositions and their petrogenetic significance. The Canadian Mineralogist 44: 599-623.

Toselli, A.; Rossi, J.; Aceñolaza, F. 1986. A proposal for the systematization of the Upper-Pre-cambrian, Lower Paleozoic basement in the Pampean Ranges, Argentina. Zentralblatt für Geologie und Paläontologie 1 (9-10): 1227-1233.

Toselli, A.; Sial, A.; Rossi, J. 2002. Ordovician magmatism of the Sierras Pampeanas, Sistema de Famatina and Cordillera Oriental, NW of Argentina. Serie de Correlación Geológica 16: 313-326.

Toselli, A.; Rossi, J.; Miller, H.; Báez, M.; Grosse, P.; López, J.; Bellos, L. 2005. Las rocas graníticas y metamórficas de la Sierra de Velasco. Serie de Correlación Geológica 19: 211-220.

Toselli, A.; Rossi, J.; Báez, M.; Grosse, P.; Sardi, F. 2006. El Batolito Carbonífero Aimogasta, Sierra de Velasco, La Rioja, Argentina. Serie de Correlación Geológica 21: 137-154.

Toselli, A.; Miller, H.; Aceñolaza, F.; Rossi, J.; Söllner, F. 2007. The Sierra de Velasco (northwestern Argentina) - an example for polyphase magmatism at the margin of Gondwana. Neues Jahrbuch für Geologie und Paläontologie 246 (7): 325-345.

Toselli, A.; Rossi, J.; Basei, M.; Larrovere, M. 2011. Controles geoquímicos e isotópicos en la petrogénesis de los granitos Devónico-Carboníferos Santa Cruz y Asha: Sierra de Velasco, Argentina. Serie Correlación Geológica 27 (2): 77-98.

Verdecchia, S.O. 2009. Las metamorfitas de baja presión vinculadas al arco magmático Famatiniano: las unidades metamórficas de la Quebrada de La Cébila y el borde oriental del Velasco. Provincia de La Rioja-Argentina. Ph.D. (Unpublished), Thesis, Universidad Nacional de Córdoba: 312 p.

Verdecchia, S.; Baldo, E. 2010. Geoquímica y procedencia de los metasedimentos ordovícicos delcomplejo metamórfico La Cébila, provincia de La Rioja, Argentina. Revista Mexicana de Ciencias Geológicas 27: 97-111.

Verdecchia, S.O.; Baldo, E.G.; Benedetto, J.L.; Borghi, P.A. 2007. The first shelly faunas from metamorphic rocks of the Sierras Pampeanas (La Cébila Formation, Sierra de Ambato, Argentina): age and paleogeographic implications. Ameghiniana 44: 493-498.

Verdecchia, S.; Casquet, C.; Baldo, E.; Pankhurst, R.; Rapela, C.; Fanning, M.; Galindo, C. 2011. Mid- to Late Cambrian docking of the Río de La Plata craton to southwestern Gondwana: age constraints from U-Pb SHRIMP detrital zircon ages from Sierras de Ambato and Velasco (Sierras Pampeanas, Argentina). Journal of the Geological Society 168: 1061-1071. London.

Vernon, R. 1986. K-feldspar megacrysts in granites phenocrysts, not porphyroblasts. Earth Science Reviews 23: 1-63.

Whalen, J.; Currie, K.; Chappell, B.1987. A-type granites: geochemical characteristics, discrimination and petrogenesis. Contribution Mineral Petrol 95: 407-419.

Manuscript received: November 28, 2016; revised/accepted: November 11, 2017; available online: January 31, 2018.